NUMERICAL SIMULATION OF THE INSTALLATION OF SUCTION BUCKETS USING MPM

M. Martinelli, Deltares, Delft, The Netherlands, +31 88 335 7210,
Mario.Martinelli@Deltares.nl
E.A. Alderlieste, Deltares, Delft, The Netherlands, +31 88 335 8417,
Etienne.Alderlieste@Deltares.nl
V. Galavi, Deltares, Delft, The Netherlands, +31 88 335 7465, Vahid.Galavi@Deltares.nl
H.J. Luger, Deltares, Delft, The Netherlands, +31 88 335 7481, Dirk.Luger@Deltares.nl

ABSTRACT

Suction buckets (or caissons) have traditionally been used for oil and gas related projects. Over the last few years, the use of suction buckets increased significantly in the offshore renewables sector. For example, 31 suction bucket jackets were installed for wind farms in the North Sea in 2018. To reduce costs, there is a need for a design optimization for this type of foundations. Experimental studies have been carried out to investigate the prediction of the installation pressure, mostly focusing on single- or two-layer soil configurations. Lab or field test experiments are sometimes extremely expensive, and they mostly focus on limited configurations, such as the dimensions of the structure and the soil type conditions. Experimental tests on complex scenarios remain very challenging. Nowadays, numerical methods demonstrate important capabilities in simulating large deformation problems such as the installation of objects. Using this technique, several experiments can be virtually reproduced with significantly less costs. This paper shows the simulation of the installation of a suction bucket using the Material Point Method (MPM). Ideal homogeneous purely cohesive and frictional soils have been investigated, and the effect of water flow has also been studied. MPM results are in good agreement with the analytical predictions, justifying the use of MPM for more complex problems.

Keywords: suction, installation, underpressure, offshore, material point method, MPM

GENERAL INTRODUCTION

In the last two decades the number of offshore wind farms has steadily grown. These wind farms typically comprise several dozen Wind Turbine Generators (WTGs) and are nowadays also installed in deeper waters. The most commonly used foundation type is a monopile. Other foundation types, such as Gravity-Based Structure (GBS) foundations and suction foundations, have been installed more often in recent years but are still limited in absolute number.

With the highly optimized monopile design and supply chain, competing on price is difficult. When challenging soil conditions are encountered, or restrictions are imposed, e.g. on noise produced during the wind farm installation, foundation options other than monopiles can become more interesting. Furthermore, hybrid wind farms comprising a combination of monopiles, GBS and suction buckets already exist (be it mainly as trials) and are likely to increase in number.

The following trends are distinguished. Wind farm developments are moving towards deeper waters and potentially more harsh environments. Hybrid wind farms with an optimized foundation type per location increase. There is more attention for better understanding and quantifying installation risks as well as the possibilities for decommissioning, see e.g. Balder et al. (2020).

Suction bucket foundations have been used in the oil and gas industry for decades and are now also accepted in the offshore wind industry. There is still room for improvements of the design, and for instance the predicted underpressures required for installation.

To reduce project uncertainties field trials can be performed, ideally combined with (back) analyses and numerical calculations. The former is rather expensive and focus in industry seems to be largely on empirical trends and numerical calculations. Developments in the numerical field are also progressing. This paper focuses on the use of the Material Point Method (MPM), which is introduced in the following section. Using MPM allows for modelling large deformations that are involved in suction bucket installation, whilst also calculating pore pressures. In the present study a single soil layer is considered. Future developments should allow for modelling installations in complex multi-layered soils that can e.g. be constructed from CPT data.

It is vital to understand the installation risks in order to further optimize foundation size and thereby costs, aiming to keep wind farm developments economically interesting in the future. MPM has the capabilities to assess pore pressure and stress development during installation and as a function of depth, which is typically challenging with existing commercial software packages.

BACKGROUND MPM

The Material Point Method is a numerical method particularly suited for large deformations with history-dependent materials. The original formulation of MPM was developed by Harlow (1964) for fluid mechanics and then applied to solid mechanics (Sulsky et al., 1995) and dry granular materials (Więckowski et al., 1999; Więckowski, 2003). Later, the method was extended to handle saturated soils (Van Esch et al., 2011) using the velocity of both solid and liquid phases as primary unknowns. It was shown that MPM is able to successfully simulate several geotechnical problems, such as cone penetration tests (Beuth & Vermeer, 2013; Ceccato & Simonini, 2015; Calvello et al., 2019), close-ended and open-ended pile installation (Phuong et al., 2016; Galavi et al., 2019), slope failure (Yerro et al., 2015), collapse of dams (Alonso & Zabala, 2011) and river banks (Bandara & Soga, 2015). In this paper, MPM is used to simulate the installation process of suction caissons.

In MPM, the continuum body is represented by a cloud of points, called Material Points (MPs). They carry all information of the continuum body, such as density, velocity, strain, stress, material parameters and external loads (Al-Kafaji, 2013). They are not physical particles, like for example single solid grains described in Discrete Element Method, but they represent a portion of the continuum body.

At the beginning of each calculation step (time step), the nodal forces are computed based on the information stored at the material points by means of the shape functions. The governing equations are then solved at degrees of freedoms in the background mesh and afterwards used to compute strains, stresses and densities, and to update the position of the material points. At the end of the time step, the mesh is reset to the original configuration (Al-Kafaji, 2013). A schematic representation of MPM and the background mesh is shown in Fig. 1.

In this paper, the saturated soils are modelled using the single-point two-phase formulation proposed by Al-Kafaji (2013) in the 2D-axisymmetric MPM (Galavi et al., 2018). The solid and fluid phases are represented by the same material point, with each phase associated to a fraction of the material point volume. The linear momentum conservations are solved for the liquid phase and for the mixture.

In case of undrained conditions, a 1-phase formulation is used to solve the momentum balance of the soil-water mixture, without the need for an extra degree of freedom of the water phase. In this case, the bulk stiffness of the water is included in the volumetric stiffness of the soil-water mixture. Since all simulations are performed underwater, the contribution of the

hydrostatic pressure is subtracted from momentum balance equations. Details of the formulation are discussed in Al-Kafaji (2013), Ceccato (2015) and Martinelli et al. (2019).

A contact formulation is defined between the caisson and soil to prevent interpenetration between the two bodies. The original frictional formulation is described in Bardenhagen et al. (2000) and it is extended including the adhesive contribution by Al-Kafaji (2013). The formulation is further improved to account for sharp edges and gap/closure between pile and soil (Galavi et al., 2019). In saturated media and in impermeable structures, the contact formulation is also used to prevent interpenetration or separation of the water phase from the structure.

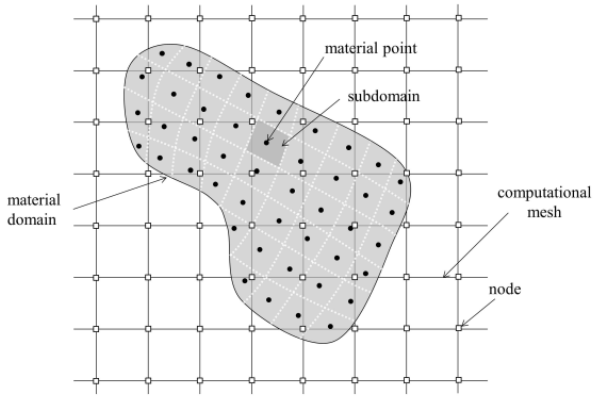

Fig. 1: Spatial discretization in MPM (Yerro, 2015).

A single computational cycle is described as follows:

a. Nodal accelerations (solid and liquid) are solved by the discretized form of the momentum balance equations (mixture and water).
b. Nodal velocities along the contact are computed from the nodal accelerations and then corrected using adhesive/frictional contact algorithm.
c. Material point velocities are computed from the nodal accelerations.
d. Nodal velocities are computed as the ratio between nodal momentum and nodal mass.
e. Strain increments, computed at the location of each material point, are used to determine the stress increment and pore pressures.
f. Positions of all material points are finally updated throughout the mesh using the solid incremental displacements.

The explicit integration scheme, as presented above, is conditionally stable. The size of a time step for a stable solution decreases with the increase of the stiffness of the material and with the decrease of the element size in the computational mesh. To reduce the computational cost, the steel caisson is modelled as a rigid body (Galavi et al., 2019). With this approach, the wave propagation is not simulated in the structure. To decrease the computational cost, the bulk modulus of water is taken equal to 20 MPa, which is 100 times smaller than the bulk modulus of pure water. It should be emphasized that the bulk modulus of natural water is significantly smaller than the bulk modulus of pure water. The used value is still large enough to ensure very limited volumetric strains in this problem and, where needed, essentially undrained behaviour.

PROBLEM DESCRIPTION

Fig. 2 shows the computational mesh and the material point distribution of the 2D-axisymmetric model. The model has a thickness of 12.5 m and a radius of 10 m. The boundary conditions are defined along the external boundary of the computational domain such that the normal velocity is zero. The caisson has a radius of 3 m and a total length of 7 m. In order to

increase the accuracy, the mesh is refined in the vicinity of the structure. In addition, the moving mesh approach (Al-Kafaji, 2013) is utilized to ensure that contact nodes on the structure and soil are always on the same coordinates to reduce oscillations in contact forces.

The material points are evenly distributed in several clusters of the computational domain to ensure that the formation of empty elements during the simulation is avoided. A set of 46 material points per element is used in the top 0.5 m of soil to have a more accurate detection of material points located along the free surface, where the pressure load is applied. Only one material point per element is used in the structure.

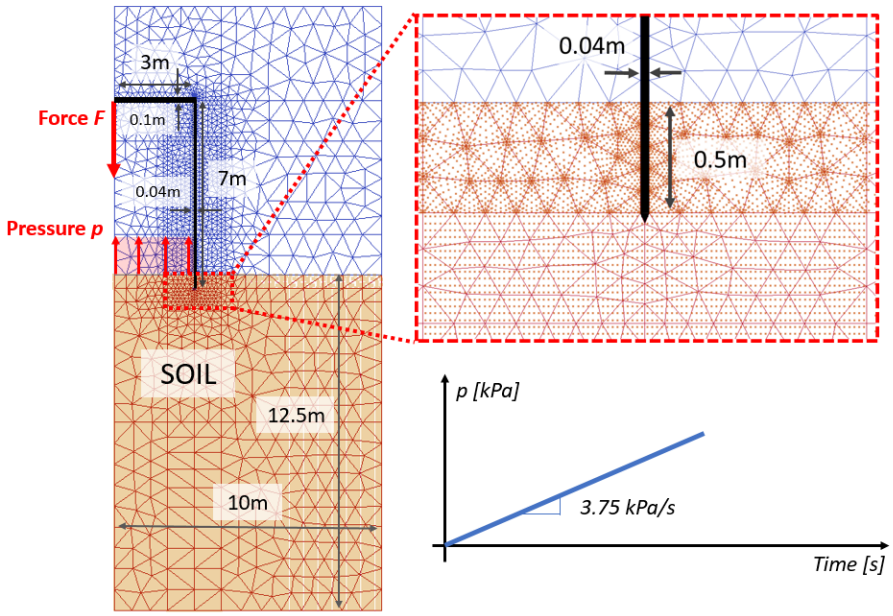

Fig. 2: Computational mesh, material point distribution and loading evolution in time.

The initial configuration is with a specified 0.5 m penetration. Then additional displacements are calculated resulting from self-weight penetration until equilibrium is met. In the following phase external loads are applied. Combined damping (Itasca, 2016) is used to mitigate the dynamic waves in the system. A damping factor of 0.25 is applied during the installation.

The installation process is simulated underwater, and it is induced by applying an under-pressure p (with respect to the hydrostatic value) inside the caisson. The effect of such a pressure is twofold. Firstly, it is a uniformly distributed over the soil surface inside the caisson as an upward traction load. The second one is that a downward force is applied directly on the structure, which is the result of the integral of the pressure over the area of the caisson.

In case of 2-phase formulation, the traction load is applied to the liquid phase and to the mixture, and it induces a water flow into the soil. Conversely, in a 1-phase undrained material, the traction load is only applied to the mixture and no water flow is induced. The water level is assumed to be deep enough to prevent the occurrence of cavitation.

A constant increase of pore pressure in time is applied during the simulation, shown in Fig. 2. It is worth noticing that such a rate is extremely fast compared to the real installation process in the field. This is admissible as long as inertia effects have no significant contribution to the process. The high rate is selected to reduce the computational time without compromising the goal of the paper, which is to show the capabilities of MPM in simulating the installation process of suction caissons.

This paper compares a suction installed caisson against a jacked (pushed in) one. The latter installation technique is simulated by applying only the downward force to the caisson, with the same rate in time as for the suction installation technique.

MATERIAL PROPERTIES

Two soil types are selected: clay and sand. An elasto-plastic model with the Mohr-Coulomb failure criterion is used for both materials. The undrained simulations are performed in the clay material, whereas the 2-phase coupled simulation is used for the sand.

An adhesive contact is used for the clay and a frictional contact for sand. The complete list of parameters is given in Table 1 and Table 2. The caisson is modelled as a rigid body with a submerged unit weight of 70 kN/m^3.

When simulating suction installation, stress oscillations are observed at the soil surface inside the caisson. They are induced by the grid-crossing of the material points with the external loads during the installation process. If the shear strength is very low, as is the case in sand at low confining stress, these stress oscillations are of the same order of magnitude as the strength, and therefore the numerical model becomes unstable. To mitigate this problem without compromising the global results, an additional surficial layer of 0.5 m of sand inside the caisson is modelled as linear elastic material instead of a Mohr-Coulomb material.

Table 1. Material properties of the clay.

Parameter	Unit	Value	Description
γ'	[kN/m^3]	9	Submerged unit weight
E'	[kPa]	8000	Young's modulus
ν	[-]	0.475	Poisson's ratio
C_u	[kPa]	50	Undrained shear strength
$C_{u,contact}$	[kPa]	10	Adhesion along contact

Table 2. Material properties of the sand.

Parameter	Unit	Value	Description
ρ_s	[kg/m^3]	2500	Density of soil grains
n	[-]	0.4	Porosity
E	[kPa]	5000	Young's modulus
ν	[-]	0.1	Poisson's ratio
c'	[kPa]	1	Cohesion
φ'	[deg]	30	Friction angle
$\varphi'_{contact}$	[deg]	20	Contact friction angle
ρ_w	[kg/m^3]	1000	Density of water
K_w	[kPa]	20000	Bulk modulus of water
k	[m/s]	1E-3	Darcy permeability

RESULTS AND DISCUSSIONS

Installation in clay under undrained condition

The results are illustrated in Fig. 3, where first the base reaction force, the internal and external shaft friction forces are plotted, and then summed-up as total reaction force. The evolution in time of the downward displacement of the caisson is also shown.

The reaction forces along the shaft (internal and external) agree with the analytical solution, which is calculated as follows:

$$F_{shaft,\text{int}} = F_{shaft,ext} = C_{u,contact} \cdot 2\pi r \cdot d_{pile} \quad (1)$$

where r is the radius of the caisson and d_{pile} is the length of the caisson embedded in the soil. The suction installation is compared against a standard jacked installation. As expected, the results show that the two installation techniques give the same reaction forces. There is no beneficial contribution of the suction inside the caisson, as there is no change in shear strength in the soil and along the contact. It is acknowledged that the tip factor for the skirt is high. This is the result of the selected coarse mesh and should be solved refining the mesh.

An additional calculation was performed with a refined mesh next to the tip (2 times) and with a larger amount of material points to avoid formation of unrealistic empty elements. Calculation time initially (using Intel i7-7th generation processor, single core and no multi-threading) was in the order of 1.5 hours, but with refined mesh increased to 2.5 hours since the size of the time step is determined by the smallest elements next to the tip. Results show a more accurate tip resistance, at a certain computational cost, and are presented in Fig. 3. Additional MPM refinements are needed to further tackle this issue.

Tip resistance using typical bearing equations equals about 200 kN. The numerical calculation with refined mesh better approaches this value. However, further mesh refinements are needed to obtain a matching result. This was not the main aim of this paper and is not further pursued.

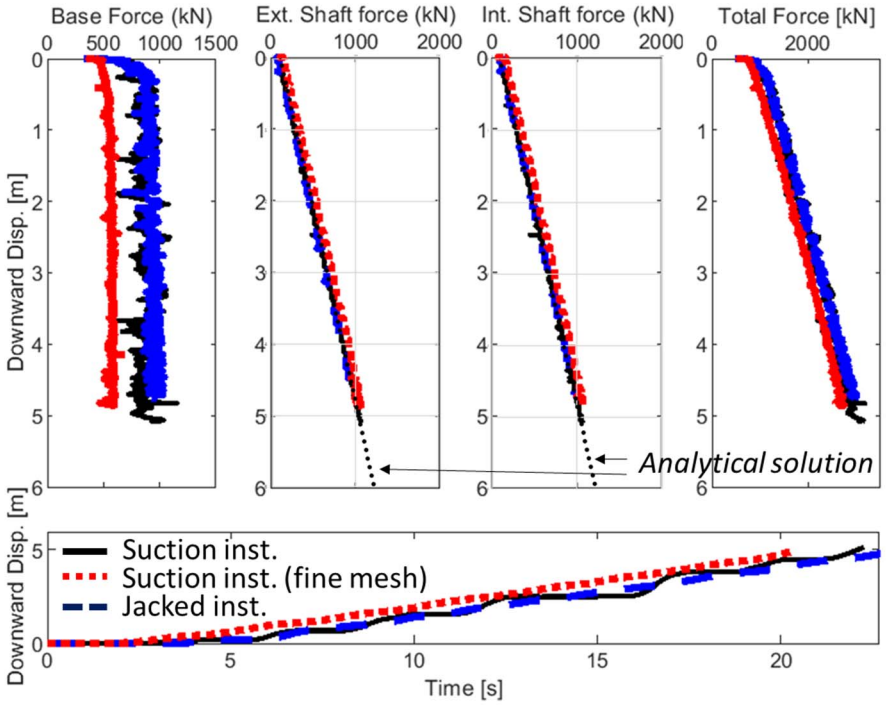

Fig. 3: Installation process in clay. Comparison between jacked and suction installation. The illustrated downward displacements are calculated after the initial equilibrium condition.

Installation in sand using coupled flow-deformation analysis

The pore pressure distribution at different time instants is shown in Fig. 4 for both installation techniques. In the suction process, a significant pore pressure gradient is induced in the soil inside the caisson. The effective stress decreases due to the generated vertical water flow, which consequently decreases the effective normal and thereby shear stress along the internal

shaft. Conversely, in case of jacked installation, no water flow is induced in the soil. Only limited excess pore pressures are generated around and at the level of the penetrating skirt tip. Outside the caisson, along the external shaft, the pore pressure remains approximately constant and similar for both installation methods.

The vertical reaction forces are illustrated in Fig. 5. In case of jacked installation, the reaction forces along the external and internal shafts are very similar. The large aspect ratio of the caisson does not allow the severe development of the arching effect inside the caisson. Only for large penetration depth, after approximately 3.7 m, the vertical reaction forces on the internal shaft surface become larger than those on the external surface, becoming only 20% higher at the end of the installation (~6 m penetration).

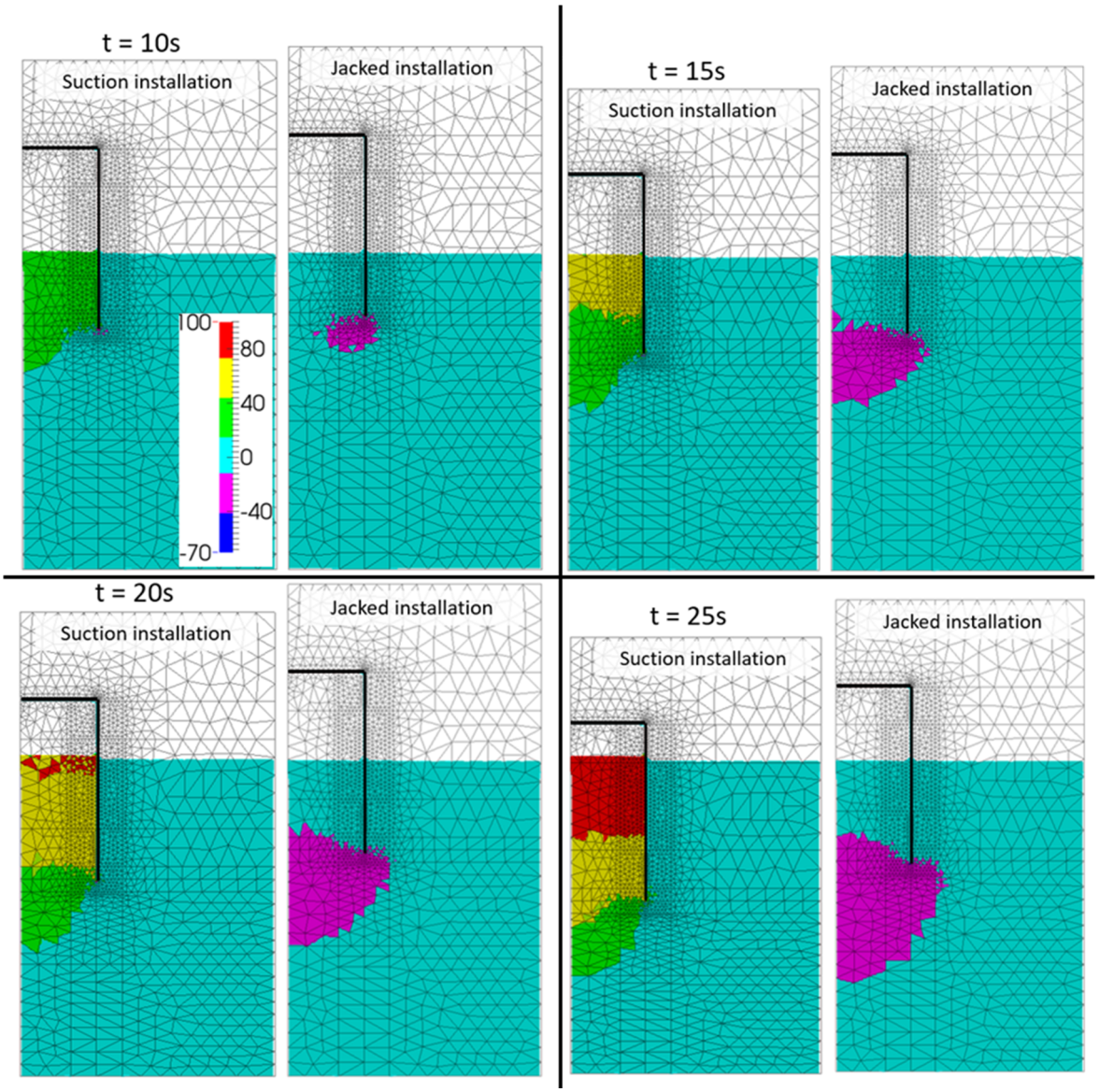

Fig. 4: Installation in sand. Excess pore pressure distribution at different time instants, for the suction and jacked installation techniques.

Comparing suction installation with jacked installation, no significant differences are observed on the external shaft surface. The reaction forces are approximately the same as those computed during a jacked installation. However, the water flow decreases drastically the internal reaction forces. They become 3.5 times lower than those computed in jacked installation. The pore pressure change also affects the bearing capacity at the base. However,

this result should be properly investigated assessing the mesh-size effect, as in this paper a very coarse mesh discretization is used at the base. Furthermore, the reduction of internal shaft friction depends on time, permeability, et cetera, and can differ for in-situ and a more realistic soil profile.

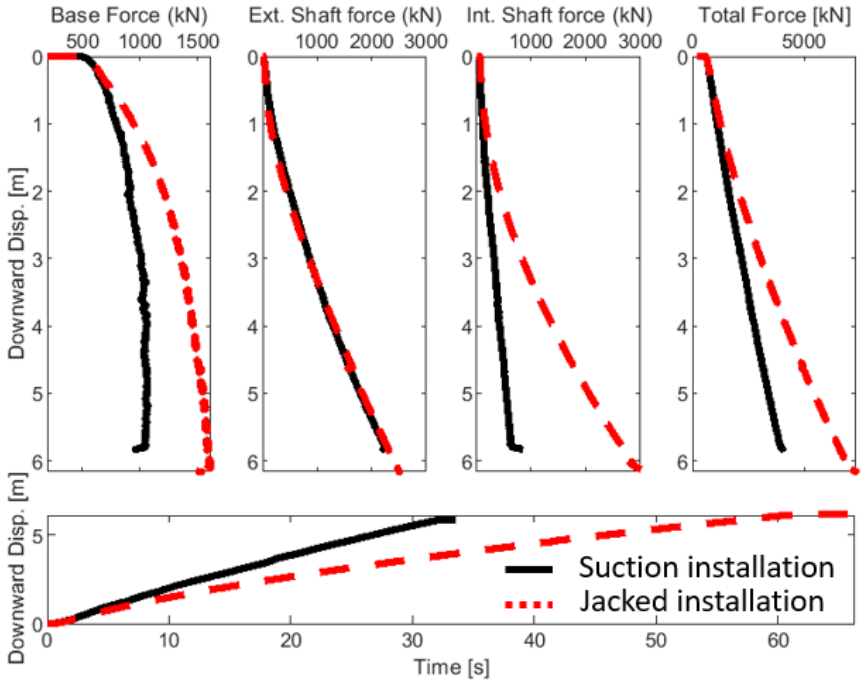

Fig. 5: Installation process in sand. Comparison between jacked and suction installation. The illustrated downward displacements are calculated after the initial equilibrium condition.

LIMITATIONS AND FUTURE WORK

As mentioned before, a relatively coarse mesh was used to limit the calculation time. A more refined mesh will be used, also to limit numerical oscillations. Furthermore, a realistic and actual case shall be back-calculated to better demonstrate MPM capabilities and functionality. For clayey soils a good example with a sensible undrained shear strength profile is given by Alderlieste & Dekker (2018).

When back-calculating actual offshore data recordings for sandy soils, the installation time and permeability have to be modelled more correctly. During offshore operations a flow of 250 m^3/h can typically be achieved, resulting in a penetration rate of about 3 m per hour for 9 to 10 m outer diameter suction foundations (and depending on losses due to ground water flow).

Commonly used installation pressure prediction methods use the measured cone resistance and soil type, implicitly allowing installation predictions in complex and layered soils. Ground water flow is, however, not yet well accounted for in design guidelines, see e.g. DNVGL (2017), Carbon Trust OWA (2019). This aim is to use MPM to further quantify installation predictions in less simplistic soil profiles.

CONCLUSIONS

The aim of this paper is to show the capabilities of the Material Point Method in modelling of the installation of suction caissons in both fine- and coarse-grained materials. The material parameters as well as the model dimensions are chosen to demonstrate features of the suction caisson installation and differences with respect to the jacked installation technique, rather than simulating a specific case.

This study illustrates that, for a clay deposit, there is no significant difference between the suction and jacked installation. In particular, the contribution of the underpressure acting on the soil surface inside the caisson is not modifying the bearing capacity of the system. On the contrary, in a sandy material, the under-pressure significantly modifies the stress distribution in the soil, especially inside the caisson, and consequently decreases the total reaction force (i.e. installation resistance) of the caisson. It is noted that a more refined mesh and an improved representation of the installation process in terms of time are required.

Even though homogenous soil profiles were selected with relatively simple constitutive models, the current framework can still be used as a solid basis to study the feasibility of the suction caisson installation, especially in conditions where complex stratigraphy makes the standard methods less applicable.

REFERENCES

Al-Kafaji, I.K.J. (2013). Formulation of a dynamic material point method (MPM) for geomechanical problems. PhD thesis, Universität Stuttgart.

Alderlieste, E.A., Dekker, M.J. (2019). Suction Pile Design and Installation Challenges for the Ophir WHP. In: Randolph M., Doan D., Tang A., Bui M., Dinh V. (Eds.) Proceedings of the 1st Vietnam Symposium on Advances in Offshore Engineering. VSOE 2018. Lecture Notes in Civil Engineering, vol 18. Springer, Singapore.

Bandara, S. and Soga, K. (2015). Coupling of soil deformation and pore fluid flow using material point method. Computers and Geotechnics 63, pp. 199-214.

Balder, T., de Lange, D.A., Elkadi, A.S.K., Egberts, P.J.P., Beuckelaers, W.J.A.P., Coronel, M., van Dijk, J., Atkinson, R., Luger, H.J., (2020). Hydraulic Pile Extraction Scale Tests (HYPE-ST): Experimental Design & Preliminary Results. In: Proceedings of the 4th International Symposium Frontiers in Offshore Geotechnics. ISFOG 2020. Austin, Texas.

Beuth, L. & Vermeer, P.A. (2013). Large deformation analysis of cone penetration testing in undrained clay, in Installation Effects in Geotechnical Engineering (M. Hicks, Ed.). Taylor & Francis Group, London, pp. 7.

Calvello, M., Ghasemi, P., Martinelli, M., Galavi, V. and Cuomo, S. (2019). In-Situ calibration of Hypoplastic model using material point method and inverse analysis, in II Int. Conf. On The Material Point Method For Modelling Soil–Water–Structure Interaction – Cambridge, UK.

Carbon Trust Offshore Wind Accelerator OWA (2019), Suction Installed Caisson Foundations for Offshore Wind: Design Guidelines, Version 1.0, February 2019.

Ceccato, F. (2015). Study of large deformation geomechanical problems with the Material Point Method. Ph.D. thesis, University of Padua.

Ceccato F., Beuth, L, Vermeer, P.A. and Simonini, P. (2016). Two-phase Material Point Method applied to cone penetration for different drainage conditions, In Geomechanics from Micro to Macro. Cambridge, pp. 965–970.

Det Norske Veritas · Germanischer Lloyd A/S, DNV·GL, (2017), Offshore soil mechanics and geotechnical engineering, DNVGL-RP-C212, August 2017.

van Esch, J., Stolle, D. and Jassim I. (2011). Finite element method for coupled dynamic flow-deformation simulation. In 2nd International Symposium on Computational Geomechanics (ComGeo II), Cavtat-Dubrovnik, Croatia, April.

Galavi, V., Martinelli, M., Elkadi, A.S.K., Ghasemi, P. and Thijssen, R. (2019). Numerical simulation of impact driven offshore monopiles using the material point method, in the XVII European Conference on Soil Mechanics and Geotechnical Engineering, Reykjavik, Iceland, 1 - 6 September 2019.

Galavi, V., Martinelli, M. and Elkadi, A.S.K. (2019). Research and Developments in JIP-SIMON project, internal report, Deltares, the Netherlands.

Galavi, V., Tehrani, F.S., Martinelli, M., Elkadi, A.S.K. and Luger, H.J. (2018). Axisymmetric formulation of the material point method for geotechnical engineering applications. Proceedings of the 9th European Conference on Numerical Methods in Geotechnical Engineering (NUMGE 2018), June 25-27, 2018, Porto, Portugal.

Itasca (2009, 2016). FLAC–Fast Lagrangian analysis of continua, v6.0, Itasca Consulting Group, Minneapolis, MN.

Martinelli, M., Luger, H.J., Talmon, A. and Galavi, V. (2019). Unstable behaviour of a sand cap placed over a weak sensitive clay deposit. CEDA Dredging Days 2019.

McKenna, G., Mooder, B., Burton, B. and Jamieson, A. (2016). Shear strength and density of oil sands fine tailings for reclamation to a boreal forest landscape, in International Oil Sands Tailings Conference, Lake Louise, Alberta, December 4 to 7, 2016.

Phuong, N.T.V., van Tol, A.F., Elkadi, A.S.K. and Rohe, A. (2016). Numerical investigation of pile installation effects in sand using material point method. Computers and Geotechnics, Vol. 73, March, pp. 58-71.

Sulsky, D., Chen Z. and Schreyer, H.L. (1994). A particle method for history-dependent materials. Computer Methods in Applied Mechanics and Engineering, Vol. 118(1-2), pp. 179–196.

Więckowski, Z. (2003). Modelling of silo discharge and filling problems by the material point method. Task Quarterly 7, No. 4, pp. 701–721.

Więckowski, Z., Youn, S.-K. and Yeon, J.-H. (1999). A particle-in-cell solution to the silo discharging problem. International Journal for Numerical Methods in Engineering, Vol. 45(9), pp. 1203–1225.

Yerro, A., Alonso, E.E. and Pinyol, N.M. (2015). The material point method for unsaturated soils. Géotechnique, 65(3), pp. 201–217.

Zabala, F. and Alonso, E.E. (2011). Progressive failure of Aznalcóllar dam using the material point method. Géotechnique, 61(9), pp. 795–808.